



---

1        **A Preliminary Assessment of the Impacts of**  
2        **Multiple Temporal-scale Variations in Particulate**  
3        **Matter on its Source Apportionment**

4

5    Xing Peng<sup>1</sup>, Jian Gao<sup>2</sup>, Guoliang Shi<sup>1\*</sup>, Xurong Shi<sup>1</sup>, Yanqi Huangfu<sup>1</sup>, Jiayuan Liu<sup>1</sup>,

6    Yuechong Zhang<sup>2</sup>, Yinchang Feng<sup>1\*\*</sup>, Wei Wang<sup>3</sup>, Ruoyu Ma<sup>3</sup>, Cesunica E. Ivey<sup>4</sup>, Yi

7    Deng<sup>5</sup>

8

9

10    <sup>1</sup>State Environmental Protection Key Laboratory of Urban Ambient Air Particulate

11    Matter Pollution Prevention and Control & Center for Urban Transport Emission

12    Research, College of Environmental Science and Engineering, Nankai University,

13    Tianjin 300350, China,

14    <sup>2</sup> Chinese Research Academy of Environmental Sciences, Beijing 100012, China,

15    <sup>3</sup> College of Software, Nankai University, Tianjin 300350, China,

16    <sup>4</sup>Department of Physics, University of Nevada Reno, Reno, Nevada, USA 89557,

17    <sup>5</sup>Earth and Atmospheric Sciences, Georgia Institute of Technology, Atlanta, GA 30332

18

19    **Correspondence to:**

20    **G.L. Shi, and Y.C. Feng,**

21    **[nksgl@nankai.edu.cn](mailto:nksgl@nankai.edu.cn);**

22    **[fengyc@nankai.edu.cn](mailto:fengyc@nankai.edu.cn)**



---

23 **Abstract.** Time series of pollutant concentrations consist of variations at different time  
24 scales that are attributable to many processes/sources (data noise, source intensities,  
25 meteorological conditions, climate, etc.). Improving the knowledge of the impact of  
26 multiple temporal-scale components on pollutant variations and pollution levels can  
27 provide useful information for suitable mitigation strategies for pollutant control during  
28 a high pollution episode. To investigate the source factors driving these variations, the  
29 Kolmogorov-Zurbenko (KZ) filter was used to decompose the time series of PM<sub>2.5</sub>  
30 (particulate matter with an aerodynamic diameter less than 2.5 μm) and chemical  
31 species into intra-day, diurnal, synoptic, and baseline temporal-scale components (TS  
32 components). The synoptic TS component has the largest amplitude and relative  
33 contributions (about 50%) to the total variance of SO<sub>4</sub><sup>2-</sup>, NH<sub>4</sub><sup>+</sup>, and OC concentrations.  
34 The diurnal TS component has the largest relative contributions to the total variance of  
35 PM<sub>2.5</sub>, NO<sub>3</sub><sup>-</sup>, EC, Ca, and Fe concentrations, ranging from 32% to 47%. To investigate  
36 the source impacts on PM<sub>2.5</sub> from different TS components, four datasets RI (intra-day  
37 removed), RD (diurnal removed), RS (synoptic removed), and RBL (baseline removed)  
38 were created by respectively removing the intra-day, diurnal, synoptic, and baseline TS  
39 component from the original datasets. Multilinear Engine 2 (ME-2) and/or principal  
40 component analysis was applied to these four datasets as well as the original datasets  
41 for source apportionment. ME-2 solutions using the original and RI dataset identify  
42 crustal dust contributions. For the solutions from original, RI, RD, and RS datasets, the  
43 total primary source impacts are close, ranging from 35.1 to 40.4 μg m<sup>-3</sup> during the  
44 entire sampling period. For the secondary source impacts, solutions from the original,



---

45 RI and RD dataset give similar source impacts (about  $30 \mu\text{g m}^{-3}$ ), which were higher

46 than the impacts derived from the RS datasets ( $21.2 \mu\text{g m}^{-3}$ ).

47 **Key words:** Multilinear Engine 2, Kolmogorov–Zurbenko filter, particulate matter,

48 temporal-scale components, source impact.

49



---

## 50 1 Introduction

51 Aerosol pollutants have become a major problem in recent years (Huang et al., 2014;  
52 van Donkelaar et al., 2015), due to its negative influences on visibility, climate change  
53 and human health (Langridge et al., 2012; Cheng et al., 2015; Butt et al., 2016; Ding et  
54 al., 2017). Variations in aerosol concentrations and chemical species reflect influences  
55 from multiple factors, such as local emissions sources and weather conditions, etc.  
56 (Keim et al., 2005). Observed concentrations of pollutants, in general, have  
57 characteristic variations, which are influenced by data noise, source intensities, short-  
58 term fluctuations, source seasonal variation, meteorological condition, climate, policy,  
59 and economic conditions (Milanchus et al., 1998; Wise and Comrie, 2005).

60 Online instruments can provide high time resolution data of particulate matter (PM)  
61 and chemical species, and these instruments have been widely applied in the detection  
62 of pollutants (Tchepel et al., 2010; Du et al., 2011; Zheng et al., 2015; Gao et al., 2016).  
63 More and more studies on aerosol pollution have become dependent on high temporal  
64 resolution observations due to their capabilities in revealing multiple temporal-scale  
65 fluctuations of the aerosol concentrations that tend to arise from different physical,  
66 chemical and dynamical processes. For example, during a high pollution period,  
67 pollutant concentrations increase rapidly by several times over a short time period, and  
68 such an increase tends to result from changing meteorological conditions. Hogrefe et  
69 al. (2000) suggested that the time series of pollutant concentrations can be decomposed  
70 into four components. The first component is the intra-day component with periods less



---

71 than 12 h and is typically linked to fast-acting, local emission sources and local-level  
72 processes (Tchepel et al., 2010). The second is the diurnal component dominated by 12-  
73 48 h periodicity. The third is the synoptic component mainly driven by 2-21 day  
74 fluctuations in weather patterns and short-term fluctuations in emissions. The last  
75 baseline component is related to the low-frequency fluctuations with periods greater  
76 than 21 days, which might including seasonal or long-term scale variation in emissions,  
77 climate, policy, etc. (Rao et al., 1997; Wise and Comrie, 2005).

78 Pollution sources are the key drivers of aerosol pollution. Understanding source  
79 impacts on aerosols is important for the control of air pollution (Zhao et al., 2017).  
80 Factor analysis models are widely used for estimating source impacts. These models  
81 include principal component analysis/multiple linear regression (PCA/MLR), Unmix,  
82 positive matrix factorization (PMF), and Multilinear Engine (ME-2) (Thurston and  
83 Spengler, 1985; Paatero and Tapper, 1994; Henry and Christensen, 2010; Yin et al.,  
84 2015; Zong et al., 2016). Among these, ME-2 is a particularly useful tool and has been  
85 widely used in source apportionment studies (Paatero, 1999; Amato et al., 2009; Peng  
86 et al., 2016). Factor analysis models depend on the variation of chemical species in  
87 aerosols (which reflects the temporal variation of sources) to extract source categories  
88 and calculate their contributions. Therefore, multiple temporal-scale variations in the  
89 raw online datasets associated with various factors (e.g., data noise and weather  
90 fluctuations) can have significant impacts on the source apportionment results using  
91 factor analysis models. This is the main motivation behind our analysis, i.e., to  
92 decompose the raw online datasets into multiple temporal-scale components and then



---

93 to estimate the influences of inclusion/exclusion of a specific temporal component on  
94 the final apportionment results.

95 The Kolmogorov–Zurbenko (KZ) filter used in our study for extraction of a  
96 specific temporal-scale component (TS component hereafter) is a low-pass filter that  
97 has been widely used for decomposing temporal variations in O<sub>3</sub>, PM, and chemical  
98 species (Rao et al., 1997; Hogrefe et al., 2000, 2006; Wise and Comrie, 2005; Tchepel  
99 et al., 2010). Hogrefe et al. (2006) reported that the synoptic component associated with  
100 synoptic scale weather fluctuations has the largest relative contribution to the total  
101 variance of hourly PM<sub>2.5</sub> concentrations, and the relative contributions of other  
102 components to total PM<sub>2.5</sub> mass concentrations varies by chemical species in PM<sub>2.5</sub>. In  
103 addition, the noise of data might impact the analysis, and efforts have been made to  
104 remove the noise (Kuebler et al., 2001; Tchepel et al., 2010; Henneman et al., 2015).  
105 Our earlier studies demonstrated that the time resolution of the data could influence the  
106 source apportionment results (Peng et al., 2016). Tchepel et al. (2010) used the KZ filter  
107 to remove noise in the PM data, fed filtered PM data into air quality models and showed  
108 that the model performance improved. In this study, we make a preliminary assessment  
109 of the impacts of multiple temporal-scale variations in PM data on source  
110 apportionment with PM<sub>2.5</sub> (PM with an aerodynamic diameter less than 2.5 μm) and its  
111 chemical species observed in Beijing, China. Wavelet analysis was first used to evaluate  
112 the periodicities of the PM and chemical species concentrations. The time series data  
113 of the PM and chemical species were then decomposed into multiple TS components  
114 using the KZ filter. Several new datasets were created by removing individual TS



---

115 components from the original receptor datasets. ME-2 or PCA analysis was conducted  
116 on the original and new datasets to assess the impacts of excluding a specific TS  
117 component on the final source apportionment results. We aim to determine what  
118 processes/sources are responsible for the main variation characteristics and overall  
119 pollution levels in this specific dataset. We also aim to determine what the implications  
120 of our results are for source apportionment analyses conducted with data from different  
121 geographical locations and under various weather/climate conditions.

## 122 2 Methods

### 123 2.1 Sampling

124 Ambient particles were collected in Beijing from 22 July 2014 to 12 August 2014 at  
125 CRAES (Chinese Research Academy of Environmental Sciences) in this research. And  
126 concentrations of PM<sub>2.5</sub>, inorganic ions, OC/EC and heavy metals were measured by β-  
127 ray monitor, model ADI 2080 online analyzer (MARGA, Applikon Analytical B.V.,  
128 The Netherlands), OC/EC analyzer (Sunset Laboratory Inc, USA) and the Xact 625  
129 automated multi-metals monitor (Copper USA), respectively, at 1 h time resolution.  
130 Twenty-three chemical species were selected for analysis, including NH<sub>4</sub><sup>+</sup>, Na<sup>+</sup>, Mg<sup>2+</sup>,  
131 Cl<sup>-</sup>, NO<sub>3</sub><sup>-</sup>, SO<sub>4</sub><sup>2-</sup>, K, Ca, Cr, Mn, Fe, Ni, Cu, Zn, As, Se, Ag, Cd, Ba, Hg, Pb, OC and  
132 EC. The principles of these instruments and QA/QC are described in detail by Gao et  
133 al. (2016).

### 134 2.2 Source Impact Model

135 ME-2, a general factor analysis model developed by Paatero (1999), was applied to



136 estimate the impacts of source categories at a location of interest. It is a general solver  
137 of widely different multilinear and quasi-multilinear problems (Ramadan et al., 2003)  
138 with the ability to deal with models consisting of a sum of products of unknowns.  
139 Instead of being restricted to a specific structure, ME-2 is defined in a “script file” that  
140 is written in a special-purpose programming language. It has efficient performance as  
141 it runs in DOS, which made it faster than those models with graphical interfaces  
142 (Ramadan et al., 2003). ME-2 decomposes original matrix  $X_{(m \times n)}$  into source impact  
143 matrix  $G_{(m \times p)}$  and source chemical species (source profile) matrix  $F_{(p \times n)}$ , as follow:

$$144 \quad X_{(m \times n)} = G_{(m \times p)} F_{(p \times n)} + E_{(m \times n)} \quad (1)$$

145 Variable  $X_{(m \times n)}$  is the chemical species concentrations (unit:  $\mu\text{g m}^{-3}$ ) in  $\text{PM}_{2.5}$  that  
146 are observed at the receptor site;  $E_{(m \times n)}$  is the residual matrix;  $m$  and  $n$  are the  
147 sample size and chemical species number, respectively; and  $p$  is the number of sources.  
148 The basic principle of ME-2 also can be expressed as follow:

$$149 \quad x_{ij} = \sum_{k=1}^p g_{ik} f_{kj} + e_{ij} \quad i = 1, 2, \dots, m \quad j = 1, 2, \dots, n \quad (2)$$

150 where  $x_{ij}$  is the element in matrix  $X_{(m \times n)}$ , which is the measured concentration of  
151 the  $j^{\text{th}}$  specie in the  $i^{\text{th}}$  sample ( $\mu\text{g m}^{-3}$ );  $g_{ik}$  is the element in matrix  $G_{(m \times p)}$  and  
152 is the impact of the  $k^{\text{th}}$  source on the  $i^{\text{th}}$  sample;  $f_{kj}$  is the element of matrix of  
153  $F_{(p \times n)}$  and is the concentration of the  $j^{\text{th}}$  specie in the  $k^{\text{th}}$  source (source profile);  
154 and  $e_{ij}$  is the element in the residual matrix (Hopke, 2003).

155 In ME-2, a priori information (e.g. chemical profiles and ratios) can be  
156 incorporated as a target to be approximately accomplished. The prior information must





157 be handled in form of auxiliary equations (Paatero, 1999). Auxiliary equations are  
158 included as additional terms  $Q_{aux}$  in an enhanced object function  $Q_{enh}$  (Amato et al.,  
159 2009; Amato and Hopke, 2012), the equation can be written as follows:

$$160 \quad Q_{enh} = Q_{main} + Q_{aux} \quad (3)$$

161 The term  $Q_{main}$  is described as follows:

$$162 \quad Q_{main} = \sum_{i=1}^m \sum_{j=1}^n (e_{ij}/\sigma_{ij})^2 \quad (4)$$

163 where  $\sigma_{ij}$  is the uncertainty in the  $j^{th}$  species for the  $i^{th}$  sample;  $e_{ij}$  has the same  
164 meaning as is described in Eq.(2).

165 One of the simplest forms of the auxiliary equation is the “pulling equation”  
166 (Paatero and Hopke, 2009), consisting of pulling  $f_{kj}$  (for instance) toward the specific  
167 target value  $a_{kj}$ :

$$168 \quad Q_{aux} = \frac{(f_{kj} - a_{kj})^2}{\sigma_{kj}^{aux2}} \quad (5)$$

169 where  $\sigma_{kj}^{aux}$  is the uncertainty connected to the pulling equation or softness of the pull;  
170 and  $f_{kj}$  is the element of factor loading. The task of ME-2 is to calculate a minimum  
171  $Q_{enh}$  value or balance the minimization of the values  $Q_{main}$  and  $Q_{aux}$  in the  
172 iterative process (Paatero and Hopke, 2009).

173 For ME-2, it requires that every element in the input dataset (matrix X) be a non-  
174 negative value. Some datasets removing TS component in this work have negative  
175 values and were analyzed using PCA instead of ME-2 due to this non-negative  
176 requirement. PCA is a useful method to qualitatively identify the pollutant sources. It  
177 reduces the number of original variables and generates a set of new variables (or called  
178 principal components) that are ordered by the contribution to the total variance in the



179 original data.

### 180 2.3 Temporal Scale Analysis

181 The KZ filter is a widely applied filtering technique due to its powerful separation  
182 characteristics, simplicity, and ability to handle missing data (Rao et al., 1997; Hogrefe  
183 et al., 2006). The principle of KZ filter is described as follow:

$$184 \quad y_t = \frac{1}{m} \sum_{s=-(m-1)/2}^{(m-1)/2} x_{(t+s)} \quad (6)$$

185  $m$  is the length of the moving average window, which is an odd number;  $x_{(t+s)}$   
186 is the  $(t + s)^{th}$  original value,  $y_t$  is the average value. Then the  $y_t$  as the input data  
187 and calculate according to Eq. (6). After  $k$  times (number of iterations) calculation,  $y_t^{(k)}$   
188 is expressed as:

$$189 \quad y_t^{(k)} = KZ_{m,k}(X) \quad (7)$$

190  $y_t^{(k)}$  is removed the variations that frequency lower than  $w$  (cutoff frequency).  
191  $k$  is the number of iterations. Before conducting the KZ filter, the data is log  
192 transformed for variance stabilization (Hogrefe et al., 2000). The separation point  $w$ ,  
193 between the high-frequency and low-frequency component, is a function of the filter  
194 parameters  $m$  and  $k$  (Rao et al., 1997). The equation can be written as follows:

$$195 \quad w \approx \frac{\sqrt{6}}{\pi} \sqrt{\frac{1-(1/2)^{1/2k}}{m^2-(1/2)^{1/2k}}} \quad (8)$$

196 Selecting proper filter parameters  $m$  and  $k$  could remove the temporal component  
197 at a specific frequency from the original dataset.

198 To select the appropriate parameters for the KZ filter, the wavelet analysis method  
199 analyzed the PM<sub>2.5</sub> and chemical species' periodicities before decomposing their



200 concentrations time series. The results of wavelet analysis suggested that the  
201 periodicities of PM<sub>2.5</sub> and chemical species are mainly 4-8 h (<12 h), 16-32 h, and 128-  
202 256 h (6-10 day) (Figure S1, see the Supporting Information), which was similar to the  
203 results reported by Hogrefe et al. (2000). This work referred to the KZ filter parameters  
204 reported by the Hogrefe et al. (2000) study, and decomposed the PM<sub>2.5</sub> and chemical  
205 species hourly concentrations into intra-day (time period less than 12 h), diurnal (12-  
206 24 h), and synoptic (2-21 days) TS components to evaluate the influence of TS  
207 components on their temporal variability. The formulas of the different TS components  
208 are as follow:

$$209 \quad X_{(intra-day)} = X_{(Original)} - e^{KZ_{3,3}\{\ln[X_{(Original)}]\}} \quad (9)$$

$$210 \quad X_{(diurnal)} = e^{KZ_{3,3}\{\ln[X_{(Original)}]\}} - e^{KZ_{13,5}\{\ln[X_{(Original)}]\}} \quad (10)$$

$$211 \quad X_{(synoptic)} = e^{KZ_{13,5}\{\ln[X_{(Original)}]\}} - e^{KZ_{103,5}\{\ln[X_{(Original)}]\}} \quad (11)$$

$$212 \quad X_{(baseline)} = X_{(Original)} - X_{(intra-day)} - X_{(diurnal)} - X_{(synoptic)} \quad (12)$$

213  $X_{(Original)}$  (original dataset) is the measured concentrations dataset including  
214 PM<sub>2.5</sub> and chemical species ( $\mu\text{g m}^{-3}$ );  $X_{(intra-day)}$ ,  $X_{(diurnal)}$ ,  $X_{(synoptic)}$ , and  
215  $X_{(baseline)}$  are concentration datasets of the intra-day, diurnal, synoptic and baseline  
216 components, respectively ( $\mu\text{g m}^{-3}$ ). The subscript numbers of KZ are descriptive  
217 parameters. For example, the first “3” in KZ<sub>3,3</sub> is the length of the moving average  
218 window, and the second “3” is the iteration time.

#### 219 **2.4 TS Component Removed Datasets**

220 To exam the impact of the four TS components on the source impacts, datasets without



221 the TS component influence were created. Four datasets were created by respectively  
222 removing the intra-day, diurnal, synoptic, and baseline TS component from the original  
223 datasets, as follow:

$$224 \quad X_{(intra-day\ removed)} = e^{KZ_{3,3}\{\ln[X_{(Original)}]\}} \quad (13)$$

$$225 \quad X_{(diurnal\ removed)} = X_{(Original)} - X_{(diurnal)} \quad (14)$$

$$226 \quad X_{(synoptic\ removed)} = X_{(Original)} - X_{(synoptic)} \quad (15)$$

$$227 \quad X_{(baseline\ removed)} = X_{(Original)} - X_{(baseline)} \quad (16)$$

228  $X_{(intra-day\ removed)}$  (RI dataset) is the concentration dataset with the intra-day  
229 TS component removed from the original dataset ( $\mu\text{g m}^{-3}$ ) and it contains the diurnal,  
230 synoptic, and baseline TS components.  $X_{(diurnal\ removed)}$  (RD dataset),  
231  $X_{(synoptic\ removed)}$  (RS dataset), and  $X_{(baseline\ removed)}$  (RBL dataset) are the datasets  
232 with the diurnal, synoptic, and baseline TS components singly removed from the  
233 original dataset, respectively. As there were many negative values in the RBL dataset,  
234 these data were analyzed by PCA to qualitatively identify the sources of  $\text{PM}_{2.5}$ . The  
235 original, RI, RD, and RS datasets were run by ME-2 for the source apportionment, and  
236 their results were compared. Also, few negative values (very low count) were replaced  
237 with a value equal to half of the detection limits. The average absolute error (AAE, see  
238 the SI) and correlation analysis were employed to compare the differences in the source  
239 impacts between original dataset and datasets with removed TS components. AAE was  
240 employed and is calculated as follows (Javitz et al., 1988):

$$241 \quad AAE_k = \frac{1}{n} \times \sum_{i=1}^n \frac{|E_{ik} - T_{ik}|}{T_{ik}} \times 100 \quad (17)$$



---

242 where,  $AAE_k$  is the  $AAE$  value for the  $k^{th}$  species and  $n$  is the number of samples.  
243  $E_{ik}$  is the concentration ( $\mu\text{g m}^{-3}$ ) of the  $k^{th}$  species for the  $i^{th}$  sample from the RI,  
244 RD, or RS datasets.  $T_{ik}$  is the concentration ( $\mu\text{g m}^{-3}$ ) of the  $k^{th}$  species for the  $i^{th}$   
245 sample from the original dataset. The larger  $AAE$  value and the lower correlation  
246 coefficients ( $r$ ) indicate a larger difference in source impacts between the original  
247 dataset and modified datasets, suggesting that the corresponding TS component has a  
248 larger influence on the observed concentrations.

### 249 **3 Result and discussion**

#### 250 **3.1 TS Component Influence on Concentrations**

251 The influence of each TS component on the pollutant concentration variation and the  
252 concentration levels were investigated. The original dataset was decomposed into intra-  
253 day, diurnal, synoptic, and baseline TS components by using the KZ filter (Figure 1).  
254 The variation analysis was then employed to study each TS component contribution to  
255 the total variance of  $\text{PM}_{2.5}$  and the chemical species concentrations (Table 1). We placed  
256 emphasis on investigating  $\text{PM}_{2.5}$  and the source markers (e.g.  $\text{SO}_4^{2-}$ , Ca, OC, etc.),  
257 because the variation of those markers can reflect the source emission pattern to some  
258 extent.

259 The sample size of the four TS components was less than original dataset, because  
260 the KZ filter was iterated with a moving average with a specified length and resulted in  
261 missing head and tail data of the original data. The same period (from 24 July 2014 to  
262 10 August 2014) of the original datasets with the same size were selected for



---

263 comparison and analysis. Among all the species,  $\text{PM}_{2.5}$  and  $\text{NO}_3^-$  had similar trends: the  
264 diurnal and synoptic TS components had larger amplitudes and higher relative  
265 contributions to the total variance of  $\text{PM}_{2.5}$  (diurnal: 36%, synoptic: 32%) and  $\text{NO}_3^-$   
266 (diurnal: 36%, synoptic: 32%) than the intra-day and baseline TS components.  $\text{SO}_4^{2-}$   
267 and  $\text{NH}_4^+$  showed similar variability: synoptic TS component had the largest amplitude  
268 and had the largest relative contributions to the total variance of  $\text{SO}_4^{2-}$  (48%) and  $\text{NH}_4^+$   
269 (54%) concentrations, followed by the baseline, diurnal and intra-day TS components.  
270 OC was relatively different from the species mentioned above. For OC, the relative  
271 contribution of the synoptic TS component was the largest (56%), followed by diurnal  
272 (23%), baseline (12%) and intra-day TS components (9%). Species from primary  
273 emission sources (such as EC, Ca, Fe, etc.) showed different patterns, compared with  
274 the secondary species ( $\text{NO}_3^-$ ,  $\text{SO}_4^{2-}$ ,  $\text{NH}_4^+$ ) discussed above. For EC and Ca, the diurnal  
275 TS component had the largest relative contribution to the total variance of  
276 concentrations, accounting for 47% and 45%, respectively. The synoptic (28%) and  
277 intra-day (40%) TS component was the second largest contributor to the total variance  
278 of EC and Ca concentrations, respectively. For Fe, diurnal and synoptic TS components  
279 had larger amplitudes and higher relative contributions to the total variance than intra-  
280 day and baseline TS components. For other elements, diurnal or intra-day TS  
281 components had the largest amplitudes and were the larger contributors to the total  
282 variance of the concentrations. Secondary organic carbon (SOC) also has been  
283 estimated using the OC/EC ratio (see Supporting Information), and the influence of TS  
284 component on the SOC was investigated (Table 1). The average concentration of SOC



---

285 was  $5.7 \pm 3.1 \mu\text{g m}^{-3}$  in this work. For SOC, the diurnal and synoptic TS components  
286 had larger amplitudes (Figure S2) and higher relative contributions to the total variance  
287 of  $\text{PM}_{2.5}$  (diurnal: 20%, synoptic: 62%). For species showing different TS component  
288 contributions, the cause was external influencing factors. For example, variability in  
289 primary species (such as Ca, EC) concentrations was mainly caused by local emission  
290 patterns and meteorological diffusion (van Pinxteren et al., 2009); secondary species  
291 were mainly influenced by chemical reaction (photochemical, liquid phase or  
292 heterogeneous reaction) and meteorological conditions (Buzcu et al., 2006; Jung et al.,  
293 2010, Martin et al., 2014). Therefore, species with similar TS component contributions  
294 trends may have similar sources or influencing factors.

295 To investigate the influence of the TS components on concentration levels, partial  
296 statistical analysis and AAE analysis were performed on the  $\text{PM}_{2.5}$  and source markers  
297 ( $\text{NO}_3^-$ ,  $\text{SO}_4^{2-}$ ,  $\text{NH}_4^+$ , Ca, Fe, OC, and EC) from five ambient datasets (including the  
298 original, RI, RD, RS, and RBL datasets). The results are shown in Figure 2 and Table  
299 S1. For ions, elements, OC/EC and  $\text{PM}_{2.5}$ , the larger gap in AAE value between the  
300 concentrations of RBL and original dataset means a larger difference between them,  
301 suggesting that the baseline TS component was the largest contributor to the average  
302 concentrations of  $\text{PM}_{2.5}$  and chemical species. The synoptic TS component also had a  
303 relatively high contribution to the average concentrations of  $\text{NO}_3^-$ ,  $\text{SO}_4^{2-}$ , and  $\text{NH}_4^+$ .  
304 The average concentrations of the three ions of the RS dataset were obviously lower  
305 and had large AAE values, compared with the results of the original dataset. For  $\text{PM}_{2.5}$   
306 and seven species, the correlation coefficients for the original dataset and RI, RD, RS,



---

307 and RBL datasets are displayed in Table S2. The lowest correlation coefficients were  
308 obtained for the RBL TS components and the original data.

309 Overall, baseline TS components dominating the average concentrations of  $PM_{2.5}$   
310 and chemical species might imply that pollutant emissions and other long-term  
311 fluctuation factors mainly determined the pollutants level in Beijing, from 22 July 2014  
312 to 12 August 2014. When synoptic, diurnal, and intra-day TS components mainly  
313 influenced the variation of  $PM_{2.5}$  and chemical species, this suggests that the short-term  
314 fluctuation (e.g. noise, weather etc.) dominantly determined the variation of pollutants.

### 315 **3.2 Source Impacts on $PM_{2.5}$ Concentrations**

316 Four datasets, including the original, RI, RD and RS datasets, were respectively  
317 introduced into ME-2 to identify the sources of  $PM_{2.5}$ . The RBL was analyzed by PCA,  
318 as several negative values were in this dataset (the ME-2 model only allows  
319 nonnegative input values). The source apportionment results were explored, including  
320 source profiles and source impacts, to investigate the source impacts on the  $PM_{2.5}$   
321 concentrations under the influence of different TS components.

322 For all four datasets, 3 to 7 factors were tested to determine the optimal number of  
323 factors (source categories). There are some criteria for choosing the appropriate number  
324 of factors, including the Q values, physical meaningfulness of the factor profiles, the  
325 reasonableness of source impacts, and goodness of fit for  $PM_{2.5}$  and chemical species  
326 concentrations. After testing, four source categories were identified using ME-2 from  
327 the original, RD, and RS datasets; five sources were obtained from the RI dataset. When





---

328 the calculated Q value close to the theoretical Q ( $Q_{the}$ ), the corresponding results might  
329 be acceptable (Hopke, 2003). The Q values of each solution calculated by ME-2 are  
330 displayed in Table S3 and were close to the theoretical Q, further suggesting that the  
331 results are acceptable.

332 Performance of ME-2 was evaluated by analyzing the goodness of fit for the  
333 modeled and measured  $PM_{2.5}$  and chemical species mass concentrations (slope, r).  
334 Figure S3 illustrates the slope and r results, respectively. For  $PM_{2.5}$ , the slopes (ranging  
335 from 1.0 to 1.1) and r (ranging from 0.8 to 1) were close to 1, suggesting the good  
336 performance of ME-2 obtained for the five runs. For original dataset run, 13 out of 23  
337 chemical species (e.g.  $SO_4^{2-}$ , OC, EC, Fe,) obtained slop values ranged from 0.80 to  
338 1.20, and r of the corresponding species were varied from 0.60 to 0.96. Other species  
339 (e.g. As, Cr, Se) obtained high slop values (larger than 1.20) and relative low r (ranged  
340 0.01 to 0.84), indicating the poor precision of modeled results for those species.  
341 Performance of solutions from RI and RD datasets are better than the solution from  
342 original dataset, due to more species obtained good slops and r values (close to 1). For  
343 RS run, slop values of chemical species range from 0.94 to 1.45, and values of six  
344 chemical species larger than 1.20. The correlation coefficients are ranged from -0.06 to  
345 0.95, which are similar with the results from the original dataset. The precision of  
346 results from BL dataset is the best than the other four runs, because slop and r values  
347 (larger than 0.89) of all species are close to 1. Summarily, receptor data filtering by KZ  
348 filter approach can improve the performance of model results obtained by ME-2.

349 For the original dataset, four factor profiles were obtained (Figure 3). Factor 1 was



---

350 characterized by Ca and Fe, which is linked to crustal dust (Pant and Harrison, 2012).  
351 Factor 2 had OC and EC, which are markers of vehicle emissions (Ramadan et al.,  
352 2003). Factor 3 was identified as coal combustion due to high loadings of OC, EC and  
353 Ca (Ramadan et al., 2003). Factor 4 was secondary formation due to elevated  $\text{SO}_4^{2-}$ ,  
354  $\text{NO}_3^-$  and  $\text{NH}_4^+$  (Pant and Harrison, 2012). According to the previous studies (Yu et al.,  
355 2013), coal combustion, secondary formation, vehicle emissions and crustal dust were  
356 the dominating sources of  $\text{PM}_{2.5}$  in Beijing. Five sources were obtained from the RI  
357 dataset, including coal combustion, crustal dust, secondary formation, secondary nitrate  
358 and vehicle emissions (Figure 3). For the RD and RS datasets, coal combustion,  
359 secondary formation, secondary nitrate and vehicle emissions were identified (Figure  
360 3), and crustal dust was not identified and was mixed with vehicle emissions from the  
361 two datasets. It was an expected result that ME-2 failed to identify the crustal dust  
362 source for the RD dataset. Because ME-2 extracts factors based on the chemical species  
363 variation pattern (the marker species variation can reflect the source emission pattern  
364 over the time), crustal dust markers (Ca and Fe) lost much variance and could not reflect  
365 the expected pattern after removing the diurnal TS component (the largest contributor  
366 to the total variance of Ca and Fe) (Table 1). As for the solution for RS dataset, the  
367 sulfate source (not the secondary formation) and the nitrate source were distinguished  
368 as different factors (Figure 3). For the solutions of the original, RI, and RD datasets,  
369 secondary formation of sulfate and nitrate source were mixed together and extracted as  
370 one factor. We found that after removing the similar part of the variance (the  
371 information filtered by KZ filter) of sulfate and nitrate, the difference between sulfate



---

372 and nitrate variation trend was more obvious, so these two sources can be distinguished  
373 by ME-2. It can be confirmed that the correlation coefficient between  $\text{NO}_3^-$  and  $\text{SO}_4^{2-}$   
374 was highest (0.86) for the synoptic TS component compared with other TS components  
375 (0.41, 0.28, and 0.82 for intra-day, diurnal, and baseline TS components, respectively).  
376 The correlation was lowest (0.49) for the RS dataset compared with other datasets (0.68,  
377 0.72, and 0.85 in the original, RI, and RD datasets, respectively).

378 The PCA results of the RBL dataset are listed in Table S4. Seven factors were  
379 extracted and accounted for 80.9% of the total variance, which had corresponding  
380 eigenvalues larger than 1 (can be considered as the potential sources). Factor 1 (19.6%  
381 of the variance) had high loadings for heavy metals, such as As, Se, Pb, etc. Factor 2  
382 had high loadings for Ca and Ba, and relatively high loadings for Mn, Fe, and EC. This  
383 factor might be associated with crustal dust and had a 14.3% contribution to the  
384 variance (Pant and Harrison, 2012). High loadings were observed for  $\text{SO}_4^{2-}$ ,  $\text{NO}_3^-$ , and  
385  $\text{NH}_4^+$  in factor 3, which is associated with secondary formation (Pant and Harrison,  
386 2012). Factor 4 had relatively high loadings for Cu and  $\text{Cl}^-$ , and factor 5 and 6 were  
387 characterized by heavy metals. After removing the baseline dataset, heavy metals and  
388 crustal dust were the dominant sources of  $\text{PM}_{2.5}$ . According to the results of the RBL  
389 dataset, we found the evidence that intra-day and diurnal TS components had larger  
390 relative contributions to the total variance of element (heavy metals) concentrations, as  
391 these elements are mainly emitted from primary sources.

392 Because there were different sample sizes for the four datasets, we selected the  
393 same period of results (from 24 July 2014 to 10 August 2014) to study the influence of



---

394 TS components on the source variation (Figure 4). The time series of source impacts  
395 from the RI, RD, and RS datasets were respectively used for correlation analysis with  
396 the corresponding results from the original dataset (Table S5). Vehicle emissions  
397 solutions from the RI ( $r = 0.45$ ) and RD ( $r = 0.51$ ) datasets had a higher correlation than  
398 the RS dataset ( $r = 0.25$ ), suggesting that intra-day and diurnal TS components had  
399 stronger influences on the source pattern (variation) of vehicle emissions. For coal  
400 combustion, results from the RI, RD, and RS datasets had similar correlation  
401 coefficients (ranging from 0.74 to 0.82). The sulfate source was identified from the RS  
402 dataset (Figure 3), however, the sulfate source had the lowest correlation with  
403 secondary formation (Table S5) solutions from the original dataset. The correlation  
404 analysis of the nitrate source produced similar results, where the lowest correlation  
405 coefficient occurred between solutions from the RS dataset and original dataset,  
406 suggesting that secondary source impact variation is dominantly affected by synoptic  
407 scale influences.

408 To further investigate source impacts on  $PM_{2.5}$  from different TS components, we  
409 discussed the average impacts of individual source categories on  $PM_{2.5}$  from the  
410 datasets with removed TS components (Table 2).

411 Vehicle emissions, crustal dust, and coal combustion were combined together for  
412 the analysis (called as TPS: total primary sources), because crustal dust was mixed with  
413 vehicle emissions and coal dust for the RD and RS datasets, as mentioned above.  
414 Secondary formation and nitrate source were also plus together for the discussion  
415 (called as TSS: total secondary sources). To better explore the influence of TS



---

416 components, source impacts during the entire sampling period and pollution period  
417 were investigated separately. For the entire sampling period, the impacts of TPS  
418 obtained from the original, RI, RD, and RS datasets were similar to each other, ranging  
419 from 35.1 to 40.4  $\mu\text{g m}^{-3}$ . This was an expected result because the intra-day, diurnal,  
420 and synoptic TS components had small influence on the concentrations levels of  
421 primary source markers (OC, EC, elements), as shown in Figure 2. The TSS solutions  
422 from the original, RI, and RD datasets exhibited similar source impacts, accounting for  
423 about 30  $\mu\text{g m}^{-3}$ , which was higher than the solution from the RS dataset (21.2  $\mu\text{g m}^{-3}$ ).  
424 The synoptic TS component had impact on the  $\text{SO}_4^{2-}$ ,  $\text{NO}_3^-$  and  $\text{NH}_4^+$  concentrations,  
425 and removing this TS component may have resulted in lower impacts of the secondary  
426 sources.

427       During the pollution period (from 30 July to 4 August 2014, gray shadow shown  
428 in Figure 1), the highest concentration of  $\text{PM}_{2.5}$  was up to 183.7  $\mu\text{g m}^{-3}$  at 1:00 am on  
429 31 July 2014, with an average concentration of 85.5  $\mu\text{g m}^{-3}$ . The TPS impacts derived  
430 from the original, RI, RD, and RS datasets were relatively stable, ranging from 30.3  $\mu\text{g}$   
431  $\text{m}^{-3}$  to 37.4  $\mu\text{g m}^{-3}$  (Table 2). The TSS impacts from the RS dataset (29.3  $\mu\text{g m}^{-3}$ ) were  
432 lower than the solutions from the original, RI, and RD runs (about 51  $\mu\text{g m}^{-3}$ ). The  
433 synoptic TS component increased the  $\text{NO}_3^-$ ,  $\text{SO}_4^{2-}$ , and  $\text{NH}_4^+$  concentrations (Figure 1),  
434 accounting for 58%, 57%, and 50% of their original average concentrations,  
435 respectively. This implies that the synoptic TS component had a larger impact on the  
436 secondary source than the primary source during the pollution period. Liu et al. (2017)  
437 reported that some haze episodes in North China Plain (including Tianjin) resulted from



---

438 elevated relative humidity (RH) and stagnant weather conditions. The study proposed  
439 an inorganic aerosol formation mechanism for which the elevated RH and the inorganic  
440 fraction increased the aerosol liquid water content (LWC), then the liquid particles  
441 would uptake pollutants to form the aerosols. In this work, elevated RH and reduced  
442 wind speeds have been observed during the pollution period (Figure S4). To further  
443 confirm the assumption, the aerosol LWC was estimated using ISORROPIA II model  
444 (Guo et al., 2015). The LWC and total ions ( $\text{NO}_3^- + \text{SO}_4^{2-} + \text{NH}_4^+$ ) depending on RH are  
445 shown in Figure S5. Under similar RH conditions, the total ions (ranged from 93 to 121  
446  $\mu\text{g m}^{-3}$ ) and LWC concentrations (ranged from 48 to 513  $\mu\text{g m}^{-3}$ ) during the pollution  
447 period were higher than the corresponding values (total ions concentrations: 22 to 38  
448  $\mu\text{g m}^{-3}$ ; LWC: concentrations 12 to 108  $\mu\text{g m}^{-3}$ ) during the non-pollution, suggesting  
449 high total ion and LWC concentrations. When the RH lower than 90% during the  
450 pollution period, the total ions concentrations remained relatively stable (about 100  $\mu\text{g}$   
451  $\text{m}^{-3}$ ), while the LWC concentrations increased. When the RH was higher than 90%, the  
452 total ions and LWC concentrations increased to 120 and 513  $\mu\text{g m}^{-3}$  during the pollution  
453 period, respectively, suggesting the drastically increasing in LWC concentrations may  
454 have led to the elevated ions concentrations. Therefore, the stagnant weather conditions  
455 and the elevated RH may increase the inorganic concentrations during the pollution  
456 period in this work.

457 Overall, removing the different TS components had little influence on primary  
458 source impact levels, suggesting that primary source impact levels were mainly  
459 influenced by the source emissions. The secondary source impact levels were mainly



---

460 influenced by synoptic influences and source emissions.

461 The BL dataset may be linked with source emissions, source seasonal variance,  
462 and long-term meteorological fluctuations. To study the source impacts from the  
463 baseline TS component, ME-2 was applied to the baseline dataset. Four sources were  
464 identified, including the nitrate source, secondary formation, coal combustion, and  
465 vehicle emissions (Figure S6). During the entire sampling period (Table 3), the average  
466 TPS and TSS impacts on  $\text{PM}_{2.5}$  mass concentrations were  $29.9 \mu\text{g m}^{-3}$  (57%) and  $22.8$   
467  $\mu\text{g m}^{-3}$  (43%) respectively. The average impacts of TPS and TSS during the pollution  
468 period were higher than the corresponding average impacts during the entire sampling  
469 period, which were  $35.6 \mu\text{g m}^{-3}$  and  $26.0 \mu\text{g m}^{-3}$ , respectively (Table 3). TPS and TSS  
470 obtained same impact percentages from the entire period and pollution period,  
471 accounting for 58% and 42% of  $\text{PM}_{2.5}$  mass concentrations, respectively. The time  
472 series of TPS, TSS, and  $\text{PM}_{2.5}$  are shown in Figure S7 and suggest that the periodicities  
473 of TPS and TSS were not synchronized. In this work, the peak of the BL TS component  
474 of  $\text{PM}_{2.5}$  was obtained when the both the TPS and the TSS impact levels were high.

#### 475 **4 Conclusions**

476 In this work, KZ filter was applied to decompose the time series of  $\text{PM}_{2.5}$  and chemical  
477 species concentrations collected in Beijing into intra-day, diurnal, synoptic, and  
478 baseline temporal-scale (TS) components. This work investigated the factors driving  
479 these variations, and influencing factors were found to vary with species. The intra-day  
480 and diurnal TS components mainly influence the fluctuation of elements concentrations



---

481 (e.g. Ca, Cr, Mn, etc); diurnal and synoptic TS components mainly impacted the  
482 fluctuation of  $PM_{2.5}$ ,  $NO_3^-$ , EC, and OC concentrations; baseline and synoptic TS  
483 components were the main factors contributing to  $SO_4^{2-}$  and  $NH_4^+$  variance. For the  
484  $PM_{2.5}$  and all chemical species concentration levels, the baseline TS component was the  
485 dominant factor.

486 To study the influence of different TS components on the source impacts on  $PM_{2.5}$ ,  
487 four datasets (RI, RD, RS, and RB) were created by removing one individual TS  
488 component from the original dataset each time. The original and the four modified  
489 datasets were analyzed by ME-2 and/or PCA, and the source apportionment results  
490 were compared. We found that removing some TS components affected the source  
491 identification. Four sources were obtained from the original and RI analyses, including  
492 crustal dust, vehicle emissions, coal combustion, and secondary formation. Crustal dust  
493 was not identified by ME-2 from the RD, RS, and BL datasets, possibly due to the fact  
494 that much of the information regarding the markers of crustal dust (e.g. Ca) was lost  
495 after removing the corresponding TS components. This suggests that the diurnal and  
496 synoptic TS components of chemical species were important for identifying the crustal  
497 dust source.

498 For the solutions from the original, RI, RD, and RS datasets, TPS (including  
499 crustal dust, vehicle emissions, and coal combustion) were similar to each other,  
500 implying that intra-day, diurnal or synoptic TS components had little influence on the  
501 TPS impact levels. The TSS (secondary formation and nitrate source) from the original,  
502 RI, and RD datasets obtained similar source impact levels; while TSS impact from the





---

503 RS dataset was lower than other three results, suggesting that TSS was mainly  
504 influenced by the synoptic TS component and source emissions. Performance of four  
505 ME-2 runs was evaluated by analyzing the goodness of fit for the modeled and  
506 measured PM<sub>2.5</sub> and chemical species mass concentrations (slope, r). Receptor data  
507 filtering intra-day TS components by KZ filter approach can improve the performance  
508 of the model and produce reasonable source impact results, suggesting that filtering  
509 noise from the instrument is useful to data analysis.

510 The major findings of this work are that during the whole sampling period and  
511 pollution period, TPS impact levels were mainly influenced by source emissions, and  
512 TSS impact levels were mainly influenced by synoptic scale weather fluctuations and  
513 source emissions. The future work will focus on the mechanism through which synoptic  
514 scale weather disturbances modulate the secondary species and sources.

515  
516 *Data availability.* The data used in this study are available from the corresponding  
517 author upon request ([nksgl@nankai.edu.cn](mailto:nksgl@nankai.edu.cn); [fengyc@nankai.edu.cn](mailto:fengyc@nankai.edu.cn)).

518 *Competing interests.* The authors declare that they have no conflict of interest.

519  
520 *Acknowledgments.* This study was supported by the National Natural Science  
521 Foundation of China (No. 41775149, 91544226), the National Key Research and  
522 Development Program of China (No. 2016YFC0208500, 2016YFC0208505), the  
523 Tianjin science and technology Foundation (No. 16YFZCSF00260), the Tianjin  
524 Natural Science Foundation (No. 17JCYBJC23000).



---

525 **References**

- 526 Amato, F., and Hopke, P. K.: Source apportionment of the ambient PM<sub>2.5</sub> across St.  
527 Louis using constrained positive matrix factorization, *Atmos. Environ.*, 46, 32-  
528 337, doi: 10.1016/j.atmosenv.2011.09.062, 2012.
- 529 Amato, F., Pandolfi, M., Escrig, A., Querol, X., Alastuey, A., Pey, J., Perez, N., and  
530 Hopke, P. K.: Quantifying road dust resuspension in urban environment by  
531 multilinear engine: a comparison with PMF2, *Atmos. Environ.*, 43, 2770-2780,  
532 doi: 10.1016/j.atmosenv.2009.02.039, 2009.
- 533 Butt, E. W., Rap, A., Schmidt, A., Scott, C. E., Pringle, K. J., Reddington, C. L.,  
534 Richards, N. A. D., Woodhouse, M. T., Ramirez-Villegas, J., Yang, H., Vakkari, V.,  
535 Stone, E. A., Rupakheti, M., Praveen, P. S., van Zyl, P. G., Beukes, J. P., Josipovic,  
536 M., Mitchell, E. J. S., Sallu, S. M., Forster, P. M., and Spracklen, D. V.: The impact  
537 of residential combustion emissions on atmospheric aerosol, human health, and  
538 climate, *Atmos. Chem. Phys.*, 16, 873-905, doi: 10.5194/acp-16-873-2016, 2016.
- 539 Buzcu, B., Yue, Z. W., Fraser, M. P., Nopmongcol, U., and Allen, D. T.: Secondary  
540 particle formation and evidence of heterogeneous chemistry during a wood smoke  
541 episode in Texas, *J. Geophys. Res.*, 111, 1485-1493, doi: 10.1029/2005JD006143,  
542 2006.
- 543 Cheng, Z., Jiang, J. K., Chen, C. H., Gao, J., Wang, S. X., Watson, J. G., Wang, H. L.,  
544 Deng, J. G., Wang, B. Y., Zhou, M., Chow, J. C., Pitchford, M. L., and Hao, J. M.:  
545 Estimation of aerosol mass scattering efficiencies under high mass loading: case



- 
- 546 study for the megacity of Shanghai, China, *Environ. Sci. Technol.*, 49, 831-838,  
547 doi: 10.1021/es504567q, 2015.
- 548 Ding, X., Zhang, Y. Q., He, Q. F., Yu, Q. Q., Wang, J. Q., Shen, R. Q., Song, W., Wang,  
549 Y. S., and Wang, X. M.: Significant increase of aromatics-derived secondary  
550 organic aerosol during fall to winter in China, *Environ. Sci. Technol.*, 51, 7432-  
551 7441, doi: 10.1021/acs.est.6b06408, 2017.
- 552 Du, H. H., Kong, L. D., Cheng, T. T., Chen, J. M., Du, J. F., Li, L., Xia, X. G., Leng, C.  
553 P., and Huang, G. H.: Insights into summertime haze pollution events over  
554 Shanghai for online water-soluble ionic composition of aerosols, *Atmos. Environ.*,  
555 45, 5131-5137, doi: 10.1016/j.atmosenv.2011.06.027, 2011.
- 556 Gao, J., Peng, X., Chen, G., Xu, J., Shi, G. L., Zhang, Y. C., and Feng, Y. C.: Insights  
557 into the chemical characterization and sources of PM<sub>2.5</sub> in Beijing at a 1-h time  
558 resolution, *Sci. Total. Environ.*, 542, 162-171, doi:  
559 10.1016/j.scitotenv.2015.10.082, 2016.
- 560 Guo, H., Xu, L., Bougiatioti, A., Cerully, K. M., Capps, S. L., Hite Jr., J. R., Carlton, A.  
561 G., Lee, S.-H., Bergin, M. H., Ng, N. L., Nenes, A., and Weber, R. J.: Fine-particle  
562 water and pH in the southeastern United States. *Atmos. Chem. Phys.*, 15, 5211-  
563 5228, doi:10.5194/acp-15-5211-2015, 2015.
- 564 Henneman, L. R. F., Holmes, H. A., Mulholland, J. A., and Russell, A. G.:  
565 Meteorological detrending of primary and secondary pollutant concentrations:  
566 Method application and evaluation using long-term (2000-2012) data in Atlanta,  
567 *Atmos. Environ.*, 119, 201-210, doi: 10.1016/j.atmosenv.2015.08.007, 2015.



- 
- 568 Henry, R. C., and Christensen, E. R.: Selecting an appropriate multivariate source  
569 apportionment model Result, *Environ. Sci. Technol.*, 44, 2474-2481, doi:  
570 10.1021/es9018095, 2010.
- 571 Hogrefe, C., Rao, S. T., Zurbenko, I. G., and Porter, P. S.: Interpreting the information  
572 in ozone observations and model predictions relevant to regulatory policies in the  
573 eastern United States, *Bull. Amer. Meteor. Soc.*, 81, 2083-2106, doi:  
574 10.1175/1520-0477(2000)081<2083:ITHIOO>2.3.CO;2, 2000.
- 575 Hogrefe, C., Porter, P. S., Gego, E., Gilliland, A., Gilliam, R., Swall, J., Irwin, J., and  
576 Rao, S. T.: Temporal features in observed and simulated meteorology and air  
577 quality over the Eastern United States, *Atmos. Environ.*, 40, 5041-5055, doi:  
578 10.1016/j.atmosenv.2005.12.056, 2006.
- 579 Hopke, P. K.: Recent developments in receptor modeling, *J. Chemometr.*, 17, 255-265,  
580 doi: 10.1002/cem.796, 2003.
- 581 Huang, R. J., Zhang, Y. L., Bozzetti, C., Ho, K. F., Cao, J. J., Han, Y. M., Daellenbach,  
582 K. R., Slowik, J. G., Platt, S., Canonaco, F., Zotter, P., Wolf, R., Pieber, S., Bruns,  
583 E. A., Crippa, M., Ciarelli, G., Piazzalunga, A., Schwikowski, M., Abbaszade, G.,  
584 Schnelle-Kreis, J., Zimmermann, R., An, Z. S., Szidat, S., Baltensperger, U.,  
585 Haddad, I. E., and Prevot, A. S. H.: High secondary aerosol contribution to  
586 particulate pollution during haze events in China, *Nature.*, 514, 218-222, doi:  
587 10.1038/nature13774, 2014.



- 
- 588 Javitz, H. S., Watson, J. G., and Robinson, N.: Performance of the chemical mass  
589 balance model with simulated local-scale aerosols, *Atmos. Environ.*, 22, 2309-  
590 2322, doi: 10.1016/0004-6981(88)90142-4, 1998.
- 591 Jung, J. S., Tsatsral, B., Kim, Y. J., and Kawamura, K.: Organic and inorganic aerosol  
592 compositions in Ulaanbaatar, Mongolia, during the cold winter of 2007 to 2008:  
593 Dicarboxylic acids, ketocarboxylic acids, and  $\alpha$ -dicarbonyls, *J. Geophys. Res.*  
594 *Atmos.*, 115, 1842-1851, doi: 10.1029/2010JD014339, 2010.
- 595 Keim, B. D., Meeker, L. D., and Slater, J. F.: Manual synoptic climate classification  
596 for the East Coast of New England (USA) with an application to  $PM_{2.5}$   
597 concentration, *Climate Res.*, 28, 143-153, doi: 10.3354/cr028143, 2005.
- 598 Kuebler, J., Bergh, H. V. D., and Russell, A. G.: Long-term trends of primary and  
599 secondary pollutant concentrations in Switzerland and their response to emission  
600 controls and economic changes, *Atmos. Environ.*, 35, 1351-1363, doi:  
601 10.1016/S1352-2310(00)00401-5, 2001.
- 602 Langridge, J. M., Lack, D., Brock, C. A., Bahreini, R., Middlebrook, A. M., Neuman,  
603 J. A., Nowak, J. B., Perring, A. E., Schwarz, J. P., and Spackman, J. R.: Evolution  
604 of aerosol properties impacting visibility and direct climate forcing in an  
605 ammonia-rich urban environment, *J. Geophys. Res. Atmos.*, 117, 2240-2260, 2012.
- 606 Liu, Y. C., Wu, Z. J., Wang, Y., Xiao, Y., Gu, F. T., Zheng, J., Tan, T. Y., Shang, D.  
607 J., Wu, Y. S., Zeng, L. M., Hu, M., Bateman, A. P., Martin, S.T.: Submicrometer  
608 particles are in the liquid state during heavy haze episodes in the urban atmosphere



- 
- 609 of Beijing, China. *Environ. Sci. Technol. Lett.*, 4 (10), 427-432, doi:  
610 10.1021/acs.estlett.7b00352, 2017.
- 611 Martin, E., Bekki, S., Ninin, C., and Bindeman, I.: Volcanic sulfate aerosol formation  
612 in the troposphere, *J. Geophys. Res. Atmos.*, 119, 660-673, doi:  
613 10.1029/2011JD017116, 2014.
- 614 Milanchus, M. L., Rao, S. T., and Zurbenko, I. G.: Evaluating the effectiveness of ozone  
615 management efforts in the presence of meteorological variability, *J. Air & Waste  
616 Manage. Assoc.*, 48, 201-215, doi.org/10.1080/10473289.1998.10463673, 1998.
- 617 Paatero, P.: The multilinear engine-A table-driven, least squares program for solving  
618 multilinear problems, including the n-way parallel factor analysis model, *J.  
619 Comput. Graph. Stat.*, 8, 854-888, doi: 10.2307/1390831, 1999.
- 620 Paatero, P., and Tapper, U.: Positive matrix factorization: a non-negative factor model  
621 with optimal utilization of error estimates of data values, *Environmetrics*, 5, 111-  
622 126, doi: 10.1002/env.3170050203, 1994.
- 623 Paatero, P., and Hopke, P. K.: Rotational tools for factor analytic models, *J. Chemom.*,  
624 23, 91-100, doi: 10.1002/cem.1197, 2009.
- 625 Pant, P., and Harrison, R. M.: Critical review of receptor modelling for particulate  
626 matter: A case study of India, *Atmos. Environ.*, 49, 1-12, doi:  
627 10.1016/j.atmosenv.2011.11.060, 2012.
- 628 Peng, X., Shi, G. L., Gao, J., Liu, J. Y., Huangfu, Y. Q., Ma, T., Wang, H. T., Zhang, Y.  
629 C., Wang, H., Li, H., Ivey, C. E., and Feng, Y. C.: Characteristics and sensitivity



- 
- 630 analysis of multiple-time-resolved source patterns of PM<sub>2.5</sub>, with real time data  
631 using Multilinear Engine 2, Atmos. Environ., 139, 113-121, doi:  
632 10.1016/j.atmosenv.2016.05.032, 2016.
- 633 Ramadan, Z., Eickhout, B. X., Song, H., Buydens, L. M. C., and Hopke, P. K.:  
634 Comparison of Positive Matrix Factorization and Multilinear Engine for the source  
635 apportionment of particulate pollutants, Chemom. Intell. Lab. Syst., 66, 15-28, doi:  
636 10.1016/S0169-7439(02)00160-0, 2003.
- 637 Rao, S. T., Zurbenko, I. G., Neagu, R., Porter, P. S., Ku, J. Y., and Henry, R. F.: Space  
638 and time scales in ambient ozone data, Bull. Amer. Meteor. Soc., 78, 2153-2166,  
639 doi: 10.1175/1520-0477(1997)078<2153:SATSIA>2.0.CO;2, 1997.
- 640 Tchepel, O., Costa, A. M., Martins, H., Ferreira, J., Monteiro, A., Miranda, A. I., and  
641 Borrego, C.: Determination of background concentrations for air quality models  
642 using spectral analysis and filtering of monitoring data, Atmos. Environ., 44, 106-  
643 114, doi: 10.1016/j.atmosenv.2009.08.038, 2010.
- 644 Thurston, G. D., and Spengler, J. D.: A quantitative assessment of source contributions  
645 to inhalable particulate matter pollution in metropolitan Boston, Atmos. Environ.,  
646 19, 9-25, doi: 10.1016/0004-6981(85)90132-5, 1985.
- 647 van Donkelaar, A., Martin, R. V., Brauer, M., and Boys, B. L.: Use of satellite  
648 observations for long-term exposure assessment of global concentrations of fine  
649 particulate matter, Environmen. Health Persp., 123, 135-143,  
650 doi.org/10.1289/ehp.1408646, 2015.
- 651 van Pinxteren, D., Brüggemann, E., Gnauk, T., Iinuma, Y., Müller, K., Nowak, A.,



- 
- 652       Achtert, P., Wiedensohler, A., and Herrmann, H.: Size- and time-resolved  
653       chemical particle characterization during CAREBeijing-2006: Different pollution  
654       regimes and diurnal profiles, *J. Geophys. Res. Atmos.*, 114, 899-912, doi:  
655       10.1029/2008JD010890, 2009.
- 656       Wise, E. K., and Comrie, A. C.: Extending the Kolmogorov–Zurbenko filter:  
657       application to ozone, particulate matter, and meteorological trend, *J. Air & Waste*  
658       *Manage. Assoc.*, 55, 1208-1216, doi.org/10.1080/10473289.2005.10464718, 2005.
- 659       Yin, J., Cumberland, S. A., Harrison, R. M., Allan, J., Young, D. E., Williams, P. I., and  
660       Coe, H.: Receptor modelling of fine particles in southern England using CMB  
661       including comparison with AMS-PMF factors, *Atmos. Chem. Phys.*, 15, 2139-  
662       2158, doi: 10.5194/acp-15-2139-2015, 2015.
- 663       Yu, L. D., Wang, G. F., Zhang, R. J., Zhang, L. M., Song, Y., Wu, B. B., Li, X. F., An,  
664       K., and Chu, J. H.: Characterization and source apportionment of PM<sub>2.5</sub> in an urban  
665       environment in Beijing, *Aerosol. Air. Qual. Res.*, 13, 574-583, doi:  
666       10.4209/aaqr.2012.07.0192, 2013.
- 667       Zhao, B., Wu, W. J., Wang, S. X., Xing, J., Chang, X., Liou, K. N., Jiang, J. H., Gu, Y.,  
668       Jang, C., Fu, J. S., Zhu, Y., Wang, J. D., Lin, Y., and Hao, J. M.: A modeling study  
669       of the nonlinear response of fine particles to air pollutant emissions in the Beijing-  
670       Tianjin-Hebei region, *Atmos. Chem. Phys.*, 17, 12031-12050, doi: 10.5194/acp-  
671       17-12031-2017, 2017.
- 672       Zheng, G. J., Duan, F. K., Su, H. Ma, Y. L., Cheng, Y., Zheng, B., Zhang, Q., Huang,  
673       T., Kimoto, T., Chang, D., Pöschl, U., Cheng, Y. F., and He, K. B.: Exploring the





---

674 severe winter haze in Beijing: the impact of synoptic weather, regional transport  
675 and heterogeneous reactions, Atmos. Chem. Phys., 15, 2969-2983,  
676 doi.org/10.5194/acp-15-2969-2015, 2015.

677 Zong, Z., Wang, X. P., Tian, C. G., Chen, Y. J., Qu, L., Ji, L., Zhi, G. R., Li, J., and  
678 Zhang, G.: Source apportionment of PM<sub>2.5</sub> at a regional background site in North  
679 China using PMF linked with radiocarbon analysis: insight into the contribution  
680 of biomass burning, Atmos. Chem. Phys., 16, 11249-11265, doi: 10.5194/acp-16-  
681 11249-2016, 2016.



---

682 **Tables**

683 **Table 1.** Relative contributions (%) of the different TS components to the total variance of PM<sub>2.5</sub>

684 and chemical species concentrations.

	NO <sub>3</sub> <sup>-</sup>	SO <sub>4</sub> <sup>2-</sup>	NH <sub>4</sub> <sup>+</sup>	OC	EC	Ca	Fe	SOC	PM <sub>2.5</sub>
Intra-day (%)	5	4	4	9	17	<b>40</b>	20	9	9
Diurnal (%)	<b>36</b>	18	17	23	<b>47</b>	<b>45</b>	<b>32</b>	<b>20</b>	<b>36</b>
Synoptic (%)	<b>32</b>	<b>48</b>	<b>54</b>	<b>56</b>	28	10	<b>32</b>	<b>62</b>	<b>32</b>
Baseline (%)	27	31	26	12	8	5	16	9	24

685



686 **Table 2.** Average source contributions to PM<sub>2.5</sub> (μg m<sup>-3</sup>) estimated by ME-2 from Beijing for the  
687 original, RI, RD, and RS datasets during the entire sampling period.

		Crustal dust	Vehicle emission	Coal combustion	TPS <sup>a</sup>	Secondary formation	Nitrate source	TSS <sup>b</sup>
During the entire sampling period	Original	14.2 (20%)	15.2 (22%)	11 (16%)	<b>40.4</b> <b>(58%)</b>	29.4 (42%)		<b>29.4</b> <b>(42%)</b>
	RI	8.6 (13%)	12.7 (19%)	18.5 (27%)	<b>39.9</b> <b>(58%)</b>	26.3 (38%)	2.3 (3%)	<b>28.7</b> <b>(42%)</b>
	RD		14.4 (22%)	20.8 (32%)	<b>35.1</b> <b>(54%)</b>	26.2 (41%)	3.2 (5%)	<b>29.4</b> <b>(46%)</b>
	RS		19.2 (32%)	19.8 (33%)	<b>39</b> <b>(65%)</b>	6.8 (11%)	14.4 (24%)	<b>21.2</b> <b>(35%)</b>
Pollution period	Original	13.5 (16%)	12.3 (14%)	7.7 (9%)	<b>33.5</b> <b>(39%)</b>	52.1 (61%)		<b>52.1</b> <b>(61%)</b>
	RI	6 (7%)	10.1 (12%)	17.9 (21%)	<b>34</b> <b>(40%)</b>	50.3 (59%)	1.0 (1%)	<b>51.2</b> <b>(60%)</b>
	RD		14.8 (18%)	15.5 (19%)	<b>30.3</b> <b>(37%)</b>	48.9 (60%)	2.5 (3%)	<b>51.4</b> <b>(63%)</b>
	RS		24.4 (37%)	13.1 (20%)	<b>37.4</b> <b>(56%)</b>	10.8 (16%)	18.5 (28%)	<b>29.3</b> <b>(44%)</b>

688 <sup>a</sup>TPS is the total contributions of crustal dust, vehicle emissions, and coal combustion. <sup>b</sup>TSS is the

689 total contributions of secondary formation and nitrate source.

690 **Table 3.** Average source contributions to PM<sub>2.5</sub> ( $\mu\text{g m}^{-3}$ ) estimated by ME-2 from the BL datasets.

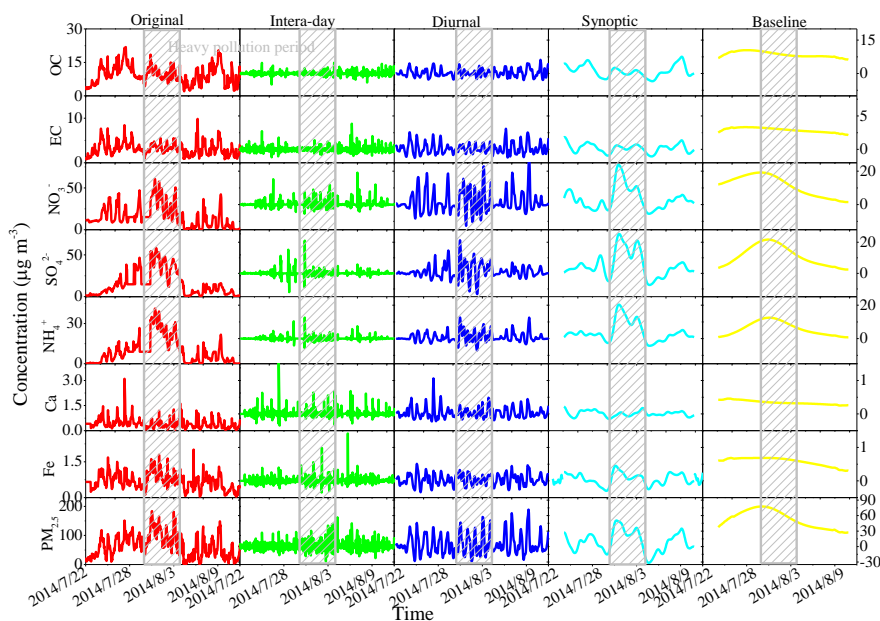
	Vehicle emission	Coal combustion	TPS <sup>a</sup>	Secondary formation	Nitrate source	TSS <sup>b</sup>
During the entire sampling period	15.4 (29%)	14.5 (28%)	<b>29.9</b> <b>(57%)</b>	12.0 (23%)	10.8 (20%)	<b>22.8</b> <b>(43%)</b>
Pollution period	17.6 (29%)	17.9 (29%)	<b>35.6</b> <b>(58%)</b>	22.4 (36%)	3.6 (6%)	<b>26.0</b> <b>(42%)</b>

691 <sup>a</sup>TPS is the total contributions of crustal dust, vehicle emissions, and coal combustion. <sup>b</sup>TSS is the

692 total contributions of secondary formation and nitrate source.

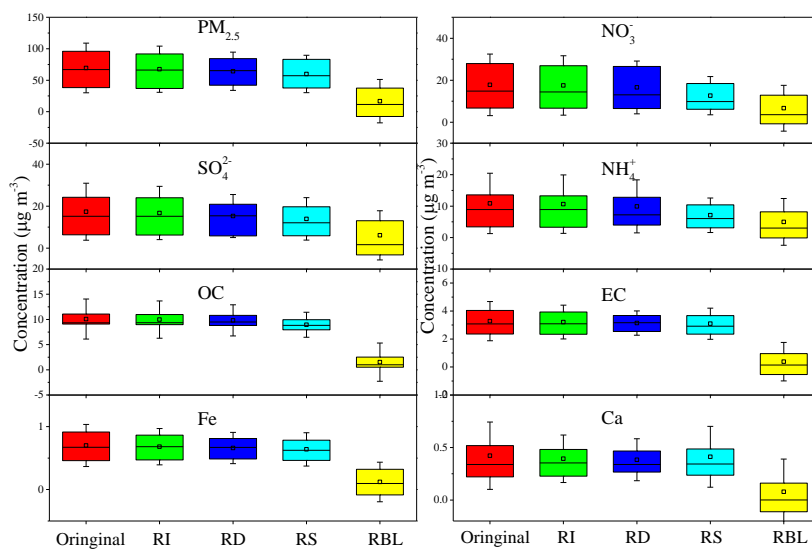


693 **Figures**



694

695 **Figure 1.** Variance of PM<sub>2.5</sub> and chemical species concentrations influenced by intra-day (time  
696 period less than 12 h), diurnal (12-24 h), synoptic (2-21 days), and baseline (greater than 21 days)  
697 temporal-scale (TS) components, for the period of 22 July 2014 to 13 Aug 2014 at Beijing, China.  
698 The variation of species that originated from primary sources mainly were influenced by diurnal TS  
699 components. The variation of ions and OC (partly from secondary formation) that originated from  
700 secondary formation mainly were influenced by synoptic TS component. The vertical gray lines  
701 demarcate the heavy pollution period.



702

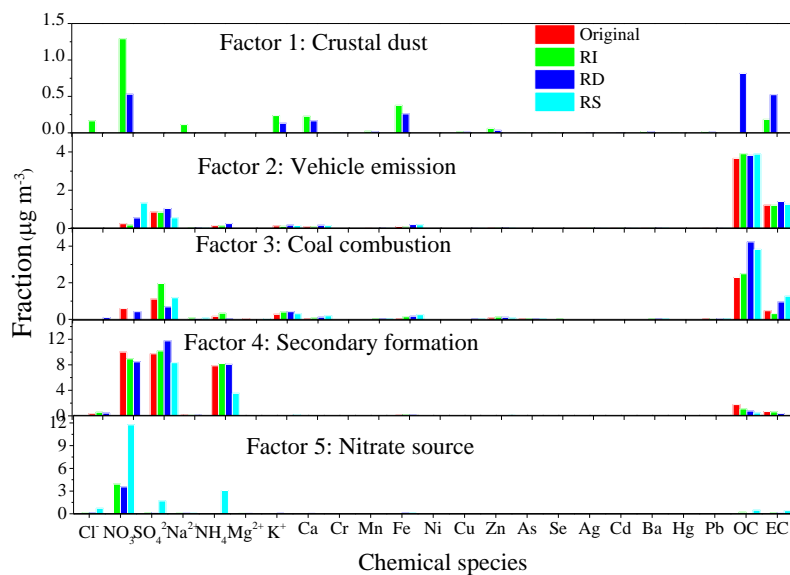
703 **Figure 2.** The influence of different TS components on the average concentrations of PM<sub>2.5</sub> and704 chemical species. The baseline TS component dominated the PM<sub>2.5</sub> and chemical species average

705 concentrations. Presented are box plots of individual chemical species from the original, RI, RD,

706 RS, and RBL datasets. Cubes denote the average and dashes denote the median concentration. The

707 whiskers are the standard deviation. (RI: intra-day removed dataset, RD: diurnal removed dataset,

708 RS: synoptic removed dataset, RBL: baseline removed dataset).



709

710 **Figure 3.** The influence of different TS components on source determination. Crustal dust was not

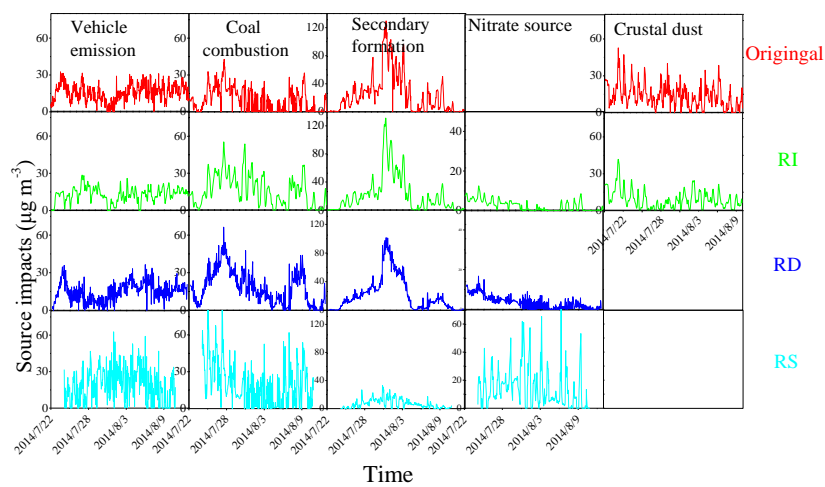
711 identified from the RD and RS datasets. Nitrate source and sulfate source were identified from the

712 RS dataset. Note: The factor 4 solution was generated from removing the synoptic dataset and

713 represents the sulfate source.



714



715

716 **Figure 4.** Source contributions to  $PM_{2.5}$  for each source (vertical columns) and each TS component

717 (horizontal rows). The blanks mean that the source has not been identified.

718